Available online at www.sciencedirect.com
SCIENCE DIRECT
Journal of Catalysis 226 (2004) 283–291
JOURNAL OF CATALYSIS
www.elsevier.com/locate/jcat

Structure and catalytic properties of molybdenum oxide catalysts supported on zirconia

Komandur V.R. Chary [a,*], Kondakindi Rajender Reddy [a], Gurram Kishan [b,1], J.W. Niemantsverdriet [b], Gerhard Mestl [c]

[a] *Catalysis Division, Indian Institute of Chemical Technology, Hyderabad-500 007, India*
[b] *Institute of Catalysis, Eindhoven University of Technology, Eindhoven, The Netherlands*
[c] *NanoScape AG, Frankfurter Ring, D-80809 Munich, Germany*

Received 10 October 2003; revised 13 April 2004; accepted 20 April 2004

Available online 2 July 2004

Abstract

MoO_3/ZrO_2 catalysts with different MoO_3 loadings (2–12 wt%) were prepared by the wet impregnation method. These catalysts were characterized by various techniques, such as X-ray diffraction (XRD), temperature-programmed reduction (TPR), laser Raman spectroscopy (LRS), X-ray photoelectron spectroscopy (XPS), and temperature-programmed desorption of NH_3 and the catalytic properties were evaluated for vapor-phase ammoxidation of toluene to benzonitrile. XRD patterns show the presence of crystalline MoO_3 peaks above 6.6 wt% MoO_3, which corresponds to the theoretical monolayer loading of MoO_3 on the zirconia used in the present study. The TPR suggests that reduction of the catalysts occurs in two stages and indicates that the reducibility of the catalysts increases with increase in MoO_3 loading up to 6.6 wt%. The acidity of the catalysts was also found to increase up to 6.6 wt% of molybdena loading and it does not increase much at higher loadings. Raman results show that the surface molybdate species are present in low-loading samples, while crystalline MoO_3 bands are observed from 9 wt% of MoO_3 and above loadings. XPS spectra showed that molybdenum was present at Mo^{6-} on all fresh samples. The Mo/Zr atomic ratio shows that the dispersion of molybdena is high below 6.6 wt% MoO_3 and dispersion decreases at higher molybdena loadings. The catalytic activity of the catalysts during ammoxidation of toluene was found to increase with loading up to 6.6 wt% and did not change appreciably beyond this loading.

Keywords: Supported molybdenum oxide catalysts; MoO_3/ZrO_2; Toluene ammoxidation; XPS; TPR; Raman spectroscopy

1. Introduction

Molybdenum oxide catalysts supported on SiO_2, Al_2O_3, and TiO_2 have been extensively investigated in the recent past. The dispersion of molybdenum oxide, its oxidation state, and structure strongly depend on the support. In turn, all these factors are likely to affect the catalytic properties. In the recent past, zirconia has attracted considerable interest because of its potential use as a catalyst support [1–8]. ZrO_2 presents special characteristics such as high thermal stability, extreme hardness, stability under reducing conditions, and both acid and base functions, which make its use very appealing as a carrier for several catalytic applications [1]. The application of zirconia as a catalyst support is promising and has been employed in many industrially important reactions such as hydroprocessing [3,5], oxidation of alcohols [6], and synthesis of methanol and higher alcohols [7–9]. Several authors have shown that the hydrotreating properties of Mo/ZrO_2 catalysts are better than those of classical supported catalysts [10–13]. The specific activity of Mo at low surface concentrations on zirconia was found to be significantly higher than that on alumina or silica. Therefore, if a sufficient amount of Mo could be dispersed at low surface coverage on zirconia, then a more active catalyst would result [14]. Strong interactions between the surfaces of zirconium oxyhydroxide precursors and dispersed metal oxides such as VO_x, MoO_x, and WO_x

* Corresponding author. Tel: +91-40-27193162, fax: +91-40-27160921.
E-mail address: kvrchary@iict.ap.nic.in (K.V.R. Chary).
[1] Present address: Chemistry and Catalysis, GE India Technology Centre, Whitefield Road, Bangalore-560066, India.

0021-9517/$ – see front matter
doi:10.1016/j.jcat.2004.04.028

lead to stable dispersed oxides, even in the presence of water at high temperatures [15,16a]. The structure of ZrO_2-supported VO_x species and their role in propane oxidative dehydrogenation (ODH) has been discussed recently, but structure–function relationships for dispersed MoO_x species remain less clear [16]. Kim et al. [17] extensively studied the molecular structures and reactivity of supported molybdenum oxides using different oxide supports prepared by the equilibrium adsorption method. The industrial importance of supported molybdenum oxide catalysts in numerous applications has prompted a large number of studies concerning the surface structures of molybdenum oxide catalysts by various techniques [18–30]. Raman spectroscopy has probably been the greatest contributor to the rapid progress in this area of catalysis because of its ability to discriminate between different metal oxide structures and its in situ capabilities.

The ammoxidation of toluene is a very important reaction for producing benzonitrile. Benzonitrile is used as a precursor for resins and coatings. It is also used as an additive in fuels and fibers [31]. Stobbelaar [31] reported the ammoxidation of toluene over supported metal oxide catalysts and concluded that MoO_3/Al_2O_3 catalysts are also of comparable importance with other vanadia-supported catalysts. MoO_3/MgF_2 catalysts were also investigated for the ammoxidation of toluene to benzonitrile [32]. Nag et al. [33] studied the partial oxidation of toluene on various supported molybdenum oxide catalysts and concluded that the activity of the catalysts was found to be high compared to molybdate salts, which in turn were more active than crystalline MoO_3. The study of molybdena-supported catalysts has also attracted some considerable interest in recent years, though traditionally, vanadia-supported catalysts have been employed for the ammoxidation of toluene [31]. In the present investigation, we report the characterization of MoO_3/ZrO_2 catalysts by XRD, TPR, LRS, XPS, and temperature-programmed desorption (TPD) of NH_3. We also report a correlation between the dispersion of molybdenum oxide and the catalytic properties of the catalysts during vapor-phase ammoxidation of toluene to benzonitrile. The purpose of this work is to study the structural and surface properties of the molybdena phase on a zirconia support.

2. Experimental methods

2.1. Catalyst preparation

A series of Mo/ZrO_2 catalysts with MoO_3 loadings in the range of 2–12 wt% was prepared by wet impregnation with ammonium heptamolybdate solution at pH 8. The ZrO_2 support (100% monoclinic zirconia with a BET surface area of 41 m^2/g) was obtained from MEL chemicals (631/01, UK) and was calcined at 500 °C for 6 h before use. After impregnation, the catalysts were dried at 110 °C for 24 h and calcined in a stream of air at 500 °C for 6 h.

2.2. X-ray diffraction

X-ray diffractograms were recorded on Siemens D-5000 diffractometer using graphite-filtered Cu-Kα radiation.

2.3. BET surface area

The BET specific surface area of the catalyst samples was measured on a Pulse Chemisorb 2700 (Micromeritics) unit by nitrogen physisorption at −196 °C.

2.4. Temperature-programmed reduction

TPR experiments were carried out on AutoChem 2910 (Micromeritics, USA) instrument. Prior to TPR, the catalyst sample was pretreated by passing ultrahigh pure (99.999%) helium (50 ml/min) at 400 °C for 2 h. After pretreatment the sample was cooled to room temperature. The carrier gas consisting of 5% hydrogen and balance argon (50 ml/min) was purified by oxy-trap and molecular sieves. The data were recorded while the temperature was ramped from ambient to 1000 °C at a heating rate of 5 °C/min. The hydrogen consumption values were calculated using GRAMS/32 software.

2.5. X-ray photoelectron spectroscopy

The X-ray photoelectron (XPS) spectra were recorded on a VG ESCALAB 200 spectrometer equipped with a dual X-ray source, of which the Al-Kα part was used, and a hemispherical analyzer, connected to a five channel detector. The background pressure during data acquisition was kept below 10^{-10} bar. Measurements were performed at 20 eV pass energy. Binding energy correction was performed by using Zr $3d_{5/2}$ peak at 182.3 eV as a reference. Spectra were fitted with the vacuum generators scientific (VGS) program fit routine. A Shirley background subtraction was applied and Gauss–Lorentz curves were used for the fits.

2.6. Laser Raman spectroscopy

The Raman spectra were recorded with a LabRam spectrometer (Dilor) equipped with a confocal microscope (Olympus) and a He–Ne laser. The slit width was usually set to 200 μm resulting together with the used 1800 grating in a spectral resolution of 2 cm^{-1}. For conventional Raman spectroscopy, the laser power of the He Ne laser attached to the LabRam spectrometer was set at 0.14 mW by neutral density filters.

2.7. Temperature-programmed desorption of ammonia

Ammonia TPD experiments were conducted on the same AutoChem 2910 instrument, which is used for TPR. Prior to TPD, the sample was pretreated by passage of high-purity (99.999%) helium (50 ml/min) at 300 °C for 1 h. After

pretreatment, the sample was saturated with high purity anhydrous ammonia from 10% NH_3 and balance He mixture (75 ml/min) at 80 °C for 1 h and subsequently flushed at 110 °C for 2 h to remove physisorbed ammonia. TPD analysis was carried out from ambient temperature to 750 °C at a heating rate of 10 °C/min. The amount of NH_3 desorbed was calculated using GRAMS/32 software.

2.8. Ammoxidation of toluene

The ammoxidation of toluene to benzonitrile reaction was carried out in a fixed-bed down-flow, cylindrical Pyrex reactor with 20-mm internal diameter. About 0.5 g of the catalyst with a 18–25 mesh size (0.5 mm) diluted with an equal amount of quartz grains of the same dimensions was charged into the reactor and supported on a glass wool bed. Prior to introduction of the reactant toluene with a syringe pump (B-Braun perfusor, Germany) the catalyst was treated in air at 400 °C for 2 h in air flow (40 ml/min) and then the reactor was fed with toluene, ammonia, and air at a mole ratio of 1:14:30. There is a preheated zone filled up with quartz glass particles heated up to 200 °C for adequate vaporization of liquid feed. The reaction products were analyzed by a HP 6890 gas chromatograph. The only by-products formed are carbon oxides during the reaction and were determined by HP-5973 GC-MS using a carbosieve column.

3. Results and discussion

Powder X-ray diffractograms of the zirconia-supported molybdenum oxide catalysts are presented in Fig. 1. Zirconia exhibits three well-established polymorphs; the monoclinic, tetragonal, and cubic phases [14]. The zirconia used in the present study is 100% monoclinic. The sharp diffraction lines at $2\theta = 24.5$, 28.3, 31.6, 34.2, 35.3, 40.7, 49.4, 50.1, and 55.4° are due to the monoclinic form of ZrO_2. No diffraction lines correspond to new phases between MoO_3 and ZrO_2. When the Mo content is low, the highly dispersed molybdenum oxide species cannot be detected by X-ray diffraction; only when the loading amount exceeds a certain extent can the residual crystalline phase of molybdenum oxide be detected. However, the possibility of MoO_3 crystallites at lower loadings having sizes less than 4 nm, which is beyond the detection capacity of XRD, cannot be ruled out.

Reflections due to the molybdenum oxide appeared from samples containing 9 wt% of MoO_3 and above loadings at $2\theta = 27.3$ and 25.7° (shown with closed circles). Calafat et al. [34] reported X-ray diffraction patterns of MoO_3/ZrO_2 catalysts and the formation of Zr $(MoO_4)_2$ at high MoO_3 contents for catalysts obtained by coprecipitation and calcined at 700 °C. It has been reported that metal oxides reduce the sintering and grain-growth rate by forming a two-dimensional layer on the surface of the zirconia particle, which reduces the mobility of defects on the grain surface or decreases the surface energy of the zirconia grain [35–37].

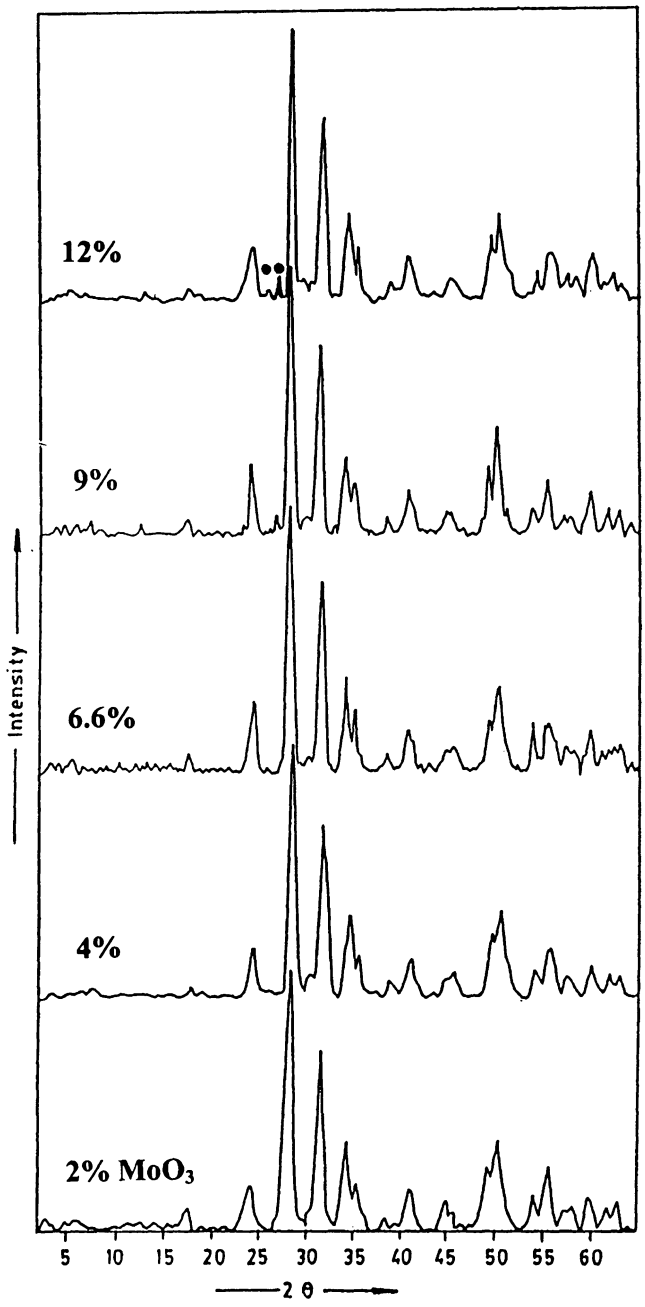

Fig. 1. X-ray diffraction patterns of various MoO_3/ZrO_2 catalysts. (•) Reflections due to MoO_3.

It can be seen from Fig. 1 that the MoO_3 crystallites start to appear from 9 wt% MoO_3.

Chen et al. [38] have shown that zirconia-supported molybdena samples can be grouped into two classes, based on the structure of the MoO_x species:

(1) $ZrMo_2O_8/ZrO_2$ samples, which consist mainly of $Zr-Mo_2O_8$ supported on ZrO_2 treated in air at 600 °C with Mo surface densities higher than 5 Mo/nm^2;
(2) MoO_x/ZrO_2 samples which consist of MoO_x species supported on ZrO_2 treated in air at 450 °C with Mo surface densities below 5 Mo/nm^2.

Table 1
Results of temperature-programmed reduction of various MoO_3/ZrO_2 catalysts

MoO_3 loading (w/w%)	BET surface area (m^2/g)	$T_{max\ 1}$ (°C)	H_2 uptake (μmol/g)	$T_{max\ 2}$ (°C)	H_2 uptake (μmol/g)	Total H_2 uptake (μmol/g)
0	41	–	–	–	–	–
2	49	425	36	940	349	385
4	50	417	100	867	714	814
6.6	50	396	211	789	990	1201
9	51	406	348	802	1188	1536
12	48	419	381	887	1487	1868

They studied the MoO_3/ZrO_2 catalysts under different treatment temperatures and also reported that the addition of small amounts of MoO_3 to ZrO_2 led to a significantly higher tetragonal content at all treatment temperatures. They also showed the presence of $ZrMo_2O_8$ in the catalysts calcined at 500 °C from XRD results. Rijnten [39] and Afanasiev et al. [40] in their studies observed that the phase transformation from monoclinic to tetragonal occurs with the impregnation of molybdenum oxide. Maity et al. [41] also observed phase transformation in their study of zirconia-supported hydrotreating catalysts. However, in the present study the monoclinic phase remained as it is even after impregnation with molybdenum oxide and no mixed oxide phase such as $ZrMo_2O_8$ is formed even at the calcination temperature of 500 °C.

The specific BET surface areas determined by nitrogen physisorption of all the catalysts are presented in Table 1. The surface area of the pure ZrO_2 sample is 41 $m^2\,g^{-1}$ and increases initially with the addition of 2 wt% molybdena loading and did not change much with further increases in molybdena loadings. The surface area of the MoO_3/ZrO_2 catalysts is more than the pure ZrO_2 in agreement with other reported results [35,42]. The theoretical monolayer capacity of MoO_3 supported on ZrO_2 has been calculated based on the method described by van Hengstum et al. [43] taking 0.16 wt% of MoO_3/m^2 of support surface. Accordingly, the theoretical monolayer capacity of MoO_3 supported on ZrO_2 employed in the present study having a surface area of 41 $m^2\,g^{-1}$ corresponds to 6.6 wt% MoO_3. The XRD results of the present work show the presence of MoO_3 crystallites from 9 wt% MoO_3. These results are further supported by X-ray photoelectron spectroscopy and laser Raman spectroscopy described in a later section.

Temperature-programmed reduction profiles of pure MoO_3 and molybdenum oxide supported on zirconia catalysts are shown in Fig. 2. The pure MoO_3 profile shows two major peaks at 767 and 997 °C and one minor reduction peak at 797 °C. The TPR analysis of pure ZrO_2 did not show any reduction peaks. For TPR analysis of unsupported MoO_3, the reduction conditions applied were similar to those applied for supported MoO_3/ZrO_2 catalysts. According to Thomas [44] and Arnoldy et al. [45] the reduction of molybdena essentially can take place in two steps. The reducibility of MoO_3 is represented by the following steps:

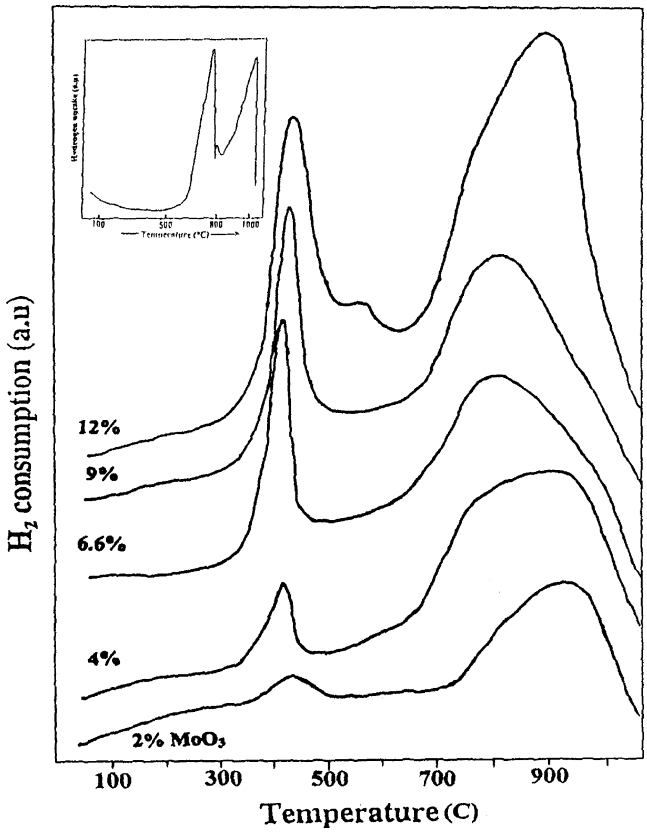

Fig. 2. Temperature-programmed reduction profiles of various pure MoO_3 and MoO_3/ZrO_2 catalysts.

$$MoO_3 \rightarrow MoO_2,$$

$$MoO_2 \rightarrow Mo.$$

The sharp peak at 767 °C corresponds to reduction of MoO_3 (first step) and the peak at 997 °C is associated with the reduction of the second step. A minor peak at the edge of the first major peak is observed at 767 °C, which corresponds to Mo_4O_{11} formed by the reduction of MoO_3. Thomas [44] noted this peak during the TPR of MoO_3 and confirmed by in situ X-ray diffraction:

$$MoO_3 \rightarrow Mo_4O_{11}.$$

The T_{max} values and the hydrogen uptake values of Mo/ZrO_2 catalysts are given in Table 1. The hydrogen uptakes were found to increase with increase in molybdena loading. TPR profiles of the Mo/ZrO_2 catalysts suggest that the reduction of molybdena occurs in two stages. It is well known that, at lower loading, molybdenum oxide is present mainly as tetrahedral species, which are difficult to reduce due to strong interaction with support. At moderate loading, both tetrahedral and octahedral species are present which are easily reducible [41]. Thus, the two peaks observed in TPR can be assigned based on the temperature at which they appear. The low-temperature peak (400–420 °C) could be assigned to the reduction of octahedral species, whereas the high

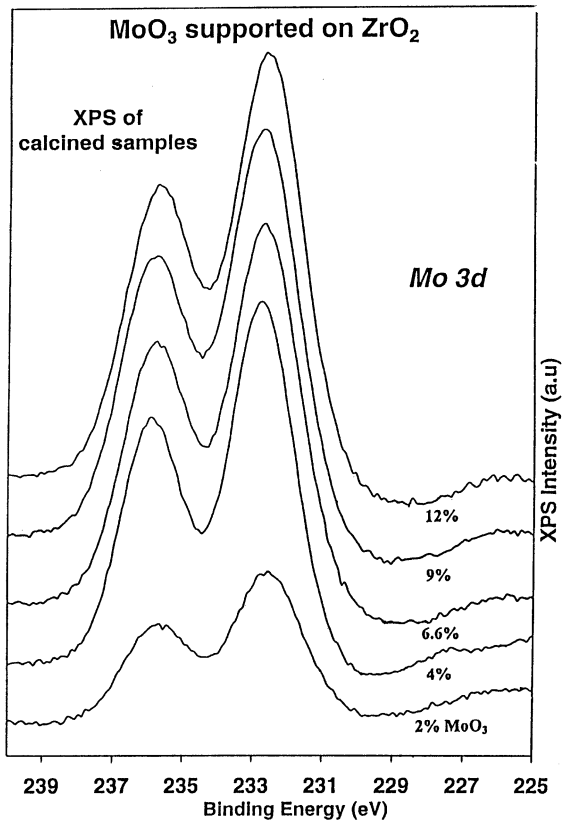

Fig. 3. Mo 3d X-ray photoelectron spectra of various MoO_3/ZrO_2 catalysts.

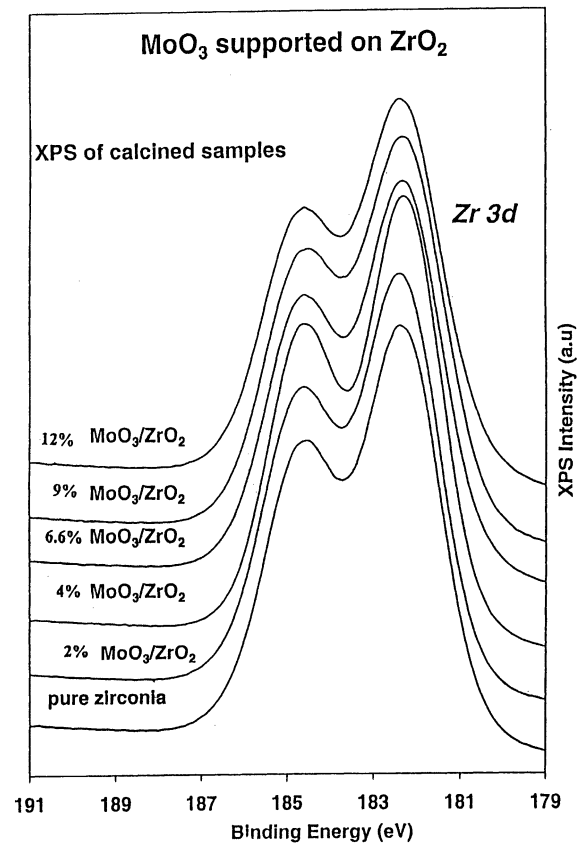

Fig. 4. Zr 3d X-ray photoelectron spectra of various MoO_3/ZrO_2 catalysts.

temperature peak (800–940 °C) may be due to reduction of tetrahedral species. Both octahedral species and crystalline MoO_3 are expected to be present at higher Mo loading. The T_{max} value of the first reduction peak was found to shift to the lower temperature side with the increase in MoO_3 loading up to 6.6 wt% of MoO_3 and found to shift to higher temperatures where MoO_3 crystallites start to appear. This clearly indicates that the dispersion of molybdena is increasing with the increase of Mo loading up to 6.6 wt% of MoO_3. The T_{max} value of the second reduction peak also shifts to lower temperatures up to 6.6 wt% and shifted to higher temperatures at higher loadings. The reduction profile of the sample with 12 wt% of MoO_3 resembles that of pure MoO_3. In a similar way the activity of the catalysts was also found to increase up to 6.6 wt% and did not change much at higher MoO_3 loadings.

Fig. 3 shows the Mo 3d XPS spectra of calcined molybdena catalysts supported on zirconia with different loadings. The major peaks around 233.0 and 235.9 eV correspond to Mo $3d_{5/2}$ and Mo $3d_{3/2}$, respectively. The reported binding energy values are those of Mo with an oxidation state of 6+ [46]. No indication for the presence of the reduced Mo ions is observed in the calcined samples. The binding energy values for all catalysts are approximately the same, which is due to the presence of one type of molybdenum oxide with the highest oxidation state (6+) in all the catalysts. This is also evidenced by the full-width at half-maximum (FWHM) values, which are in between 2.2–2.4 eV pointing to a single state (Table 2). The spectrum essentially contains one doublet at 232.7 (0.1) eV binding energy and corresponds to supported molybdenum oxo species in the highest oxidation state [28–30,47–51]. With the increase in the molybdenum loading, the intensity for the molybdenum peaks also increases.

Table 2
X-ray photoelectron spectroscopy results of various MoO_3/ZrO_2 catalysts

MoO_3 loading (wt%)	Position and FWHM of Mo $3d_{5/2}$	Position and FWHM of Zr $3d_{5/2}$
2.0	232.6 (2.3)[a]	182.3 (2.0)[a]
4.0	232.7 (2.2)	182.3 (1.9)
6.6	232.7 (2.3)	182.3 (2.1)
9.0	232.7 (2.4)	182.3 (2.2)
12.0	232.6 (2.3)	182.3 (2.2)

[a] The numbers in parentheses are FWHM values.

In Fig. 4, pure zirconium oxide (ZrO_2) and molybdena supported on zirconium oxide catalysts show similar Zr $3d_{5/2}$ binding energy values around 182.3 eV. Table 2 reports the binding energies of Zr $3d_{5/2}$ and its FWHM values (between 1.9 and 2.2), which do not change much with different molybdena loadings. The constant FWHM values, implying that only one type of doublet is present, which provides evidence for the presence of one type of zirconium oxide with an oxidation state of 4+.

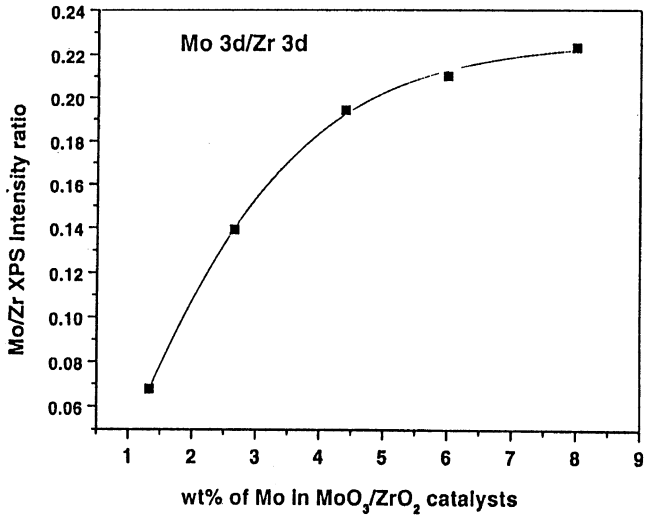

Fig. 5. Relation between Mo 3d/Zr 3d XPS intensity ratio and MoO_3 loading.

Fig. 5 shows the relation between the XPS intensity ratio Mo_{3d}/Zr_{3d} with the Mo loading in the samples. The Mo_{3d}/Zr_{3d} ratio indirectly gives the information about the dispersion of molybdenum oxide on zirconia support. The Mo/Zr atom ratio increases regularly with the molybdena loading higher than 6.6 wt%, which indicates a very high dispersion of molybdena. At higher loadings the further increase in Mo/Zr ratio is less, which indicates the formation of agglomerates and crystallites as evidence. Thus, the results indicate that at low Mo loadings dispersion is high and at higher Mo loadings the dispersion decreases [52].

The laser Raman spectra of molybdenum oxide catalysts supported on zirconia are shown in Fig. 6. Bands due to crystalline MoO_3 are seen from 9 wt% MoO_3 and the intensity of MoO_3 peaks increases with further increase of molybdena loadings. These findings are in agreement with XRD results. In the 4 wt% MoO_3 sample a peak at 920 cm^{-1} is observed which is attributed to surface molybdena species, and is found to shift to $\sim$ 950 cm^{-1}. The intensity of this peak is found to increase with MoO_3 loading. The bands in the region 900–1000 cm^{-1} are attributable to the stretching vibration of the terminal Mo=O bond of polymolybdate on ZrO_2. In the present study the Raman band of the Mo=O-stretching vibration was shifted from 920 to 950 cm^{-1}. Miyata et al. [3] reported similar results for low loaded samples. Hu et al. [53] also reported a shift to 952 cm^{-1} for 5 wt% MoO_3, which was interpreted in line with literature as due to hepta- and octamolybdates. In a recent review, Mestl and Srinivasan [54] discussed the laser Raman spectroscopy of various supported molybdenum oxide catalysts under different conditions. Ono et al. [55] investigated the structure of Mo/ZrO_2 catalysts by FT-IR and laser Raman spectroscopy. Catalysts containing 1–20 mol% MoO_3 were impregnated, dried, and calcined at 447 °C. A finely ground equimolar mixture of MoO_3 and ZrO_2 calcined at 647 °C was also investigated. At low Mo content, the surface oxide

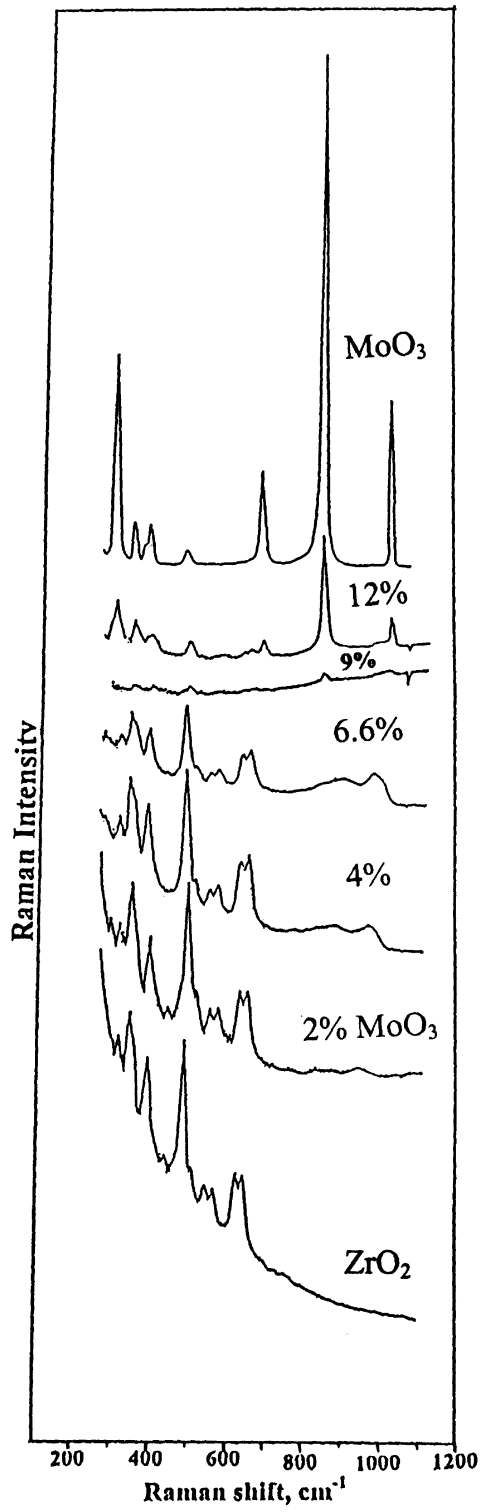

Fig. 6. Laser Raman spectra of various MoO_3/ZrO_2 catalysts recorded under ambient conditions.

was highly dispersed on ZrO_2 and present as polymolybdates. Bands due to crystalline MoO_3 are seen above 5 wt% of MoO_3 in agreement with XRD. In the physical mixture of MoO_3 and ZrO_2 the formation of $ZrMo_2O_8$ is seen in the samples calcined between 547 and 647 °C at 800, 920, and

980 cm^{-1}. Hu et al. [53] carried out a comparative study on Mo supported on different oxides, including ZrO_2. Under ambient conditions, bands at 924–951 cm^{-1} and shoulders at 880 cm^{-1} were observed to increase in frequency and intensity with Mo loading. The support band exhibited the opposite behavior, its intensity decreased with Mo loading similar to the present work. The band at 924 cm^{-1} for 1 wt% MoO_3 was attributed to MoO_4^{2-}. Alternatively, its high position may be considered as an indication of dimer formation [56]. The shift to 952 cm^{-1} for 5 wt% MoO_3 was interpreted in line with literature as due to hepta- and octamolybdates. The oxygen anion of the terminal Mo=O bond is exposed to the ambient atmosphere and easily interacts with moisture, resulting in the formation of hydrated surface species. When the MoO_3 loading is low, only isolated molybdenum oxide species, or say monomolybdate species, exist on the surface of zirconia with their Raman band around 920 cm^{-1}. With the increase of MoO_3 loading, more vacant sites are occupied, and polymerized molybdenum oxide species gradually show up due to the linkage or the combination of the neighboring monomolybdate species. In fact, the mono or polymolybdate species often irregularly distort due to their interaction with the surface of support. The distortion and different extent of interaction among surface molybdenum-oxygen species should be responsible for the large width and big shift of the terminal Mo=O Raman-stretching bands as compared with the spectra of species in solution [57]. On the other hand, Chan et al. [58] have reported that such a shift is suitable to the coordination of water molecules on the surface oxide species; i.e., at lower coverages the surface oxide species are coordinated to more water molecules than at higher coverages. In the present study as the spectra were recorded on the hydrated samples, the shift in the wavenumber to higher values seems to arise from the chain of polymolybdates on ZrO_2. From the LRS results it is clear that the MoO_3 bands are seen above 6.6 wt% loading only, which is in good agreement with the theoretical monolayer capacity and also with the XRD results. As monolayer completes at 6.6 wt% MoO_3, the ZrO_2 bands cannot be seen above this loading, above monolayer loadings only MoO_3 bands are seen (Fig. 6).

Temperature-programmed desorption of probe molecules like ammonia and pyridine is a popular method for the determination of acidity of solid catalysts as well as acid strength. In the present investigation the acidity measurements have been carried out by the ammonia TPD method. The temperature-programmed desorption profiles of the catalysts are presented in Fig. 7. The acidity values and temperature positions are given in Table 3. From the peak positions it is clear that the acidity corresponds to desorption of NH_3 in two regions associated with moderate (255–312 °C) and strong (400–430 °C) acidic sites. Strong acidic sites predominate at lower loadings and the ammonia desorption temperature shifted to a lower temperature range from 6.6 wt% MoO_3 and above loadings. The pure ZrO_2 is found to have medium acidic sites. The acidity increases with increase in molybdena loading on ZrO_2 support up to 6.6 wt% and does not increase much at higher loadings. The increase in acidity at lower loadings of the catalysts is due to the molybdena phase since ammonia uptake increases with increase in molybdena loading. The conversion values during ammoxidation of toluene to benzonitrile are also found to increase up to 6.6% MoO_3 and leveled off at higher loadings in similar lines to acidity measurements (Fig. 8). Thus the strong acidic sites might be responsible for activity during ammoxidation of toluene reaction.

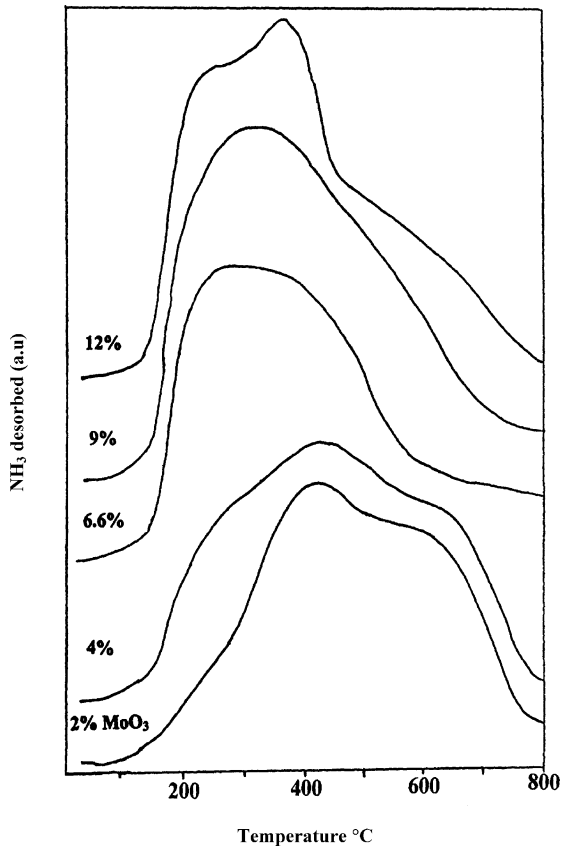

Fig. 7. Temperature-programmed desorption profiles of MoO_3/ZrO_2 catalysts.

Table 3
Results of temperature-programmed desorption (TPD) of ammonia of various MoO_3/ZrO_2 catalysts

MoO_3 loading on ZrO_2 (wt%)	T_{max} (°C)	NH_3 uptake (μmol/g)
0.0	312	120
2.0	409	273
4.0	427	345
6.6	255	368
9.0	285	369
12.0	390	370

Fig. 8 shows the relation between conversion/selectivity and rate of toluene with MoO_3 loading on ZrO_2 at 400 °C. The conversion and selectivity values were found to increase with MoO_3 loading up to 6.6 wt% of MoO_3 and leveled off

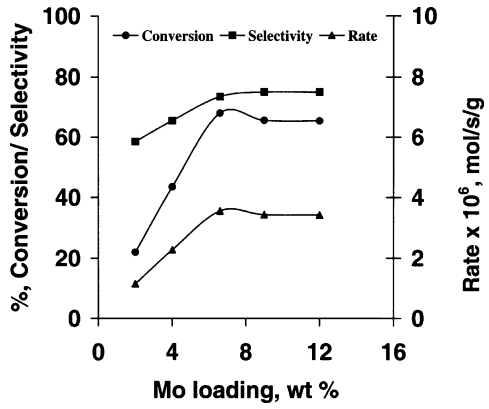

Fig. 8. Results of ammoxidation of toluene over various MoO_3/ZrO_2 catalysts. Catalyst wt, 0.5 g; reaction temperature, 400 °C; feed rate, 1 ml/h. Toluene, ammonia, and air at a mole ratio of 1:14:30.

Table 4
Activity of various supported molybdenum oxide catalysts in the ammoxidation of toluene to benzonitrile

Catalyst	Conversion (%)	Selectivity (%)
9% Mo/ZrO_2	65	71
9% Mo/TiO_2 (Degussa, P-25)	53	72
9% Mo/Nb_2O_5	62	67

at higher MoO_3 loadings. At higher loadings the selectivity increased but the increase is mild. The leveling off in activity of the catalysts beyond 6.6 wt% is due to the formation of bulk MoO_3 crystallites. XRD, LRS, and NH_3 TPD also supported the activity results. The rate was found to increase with the increase of MoO_3 loading up to 6.6 wt% and remained constant with further increase of molybdena loadings. Table 4 shows the activity of various supported molybdenum oxide catalysts in comparison to the present study. The activity results reported in Table 4 are the results from our laboratory under similar experimental conditions as those employed for Mo/ZrO_2 catalysts. The activity results of Mo/ZrO_2 catalysts are better than Mo/TiO_2 catalysts [59] and compared with Mo/Nb_2O_5 [60] catalysts. The probable mechanism involves oxidized toluene being stabilized on the catalyst surface as benzoate ion, the adsorbed benzoate ion then reacting with ammonia to form benzonitrile. The reduced centers present on MoO_3 would easily be reoxidized with molecular oxygen [31]. The ammoxidation activity of pure ZrO_2 support is found to be negligible ($< 3\%$) under similar experimental conditions as those used for the Mo/ZrO_2 catalysts. The ammoxidation activity of molybdena-supported catalysts is mainly due to the presence of surface redox and acidic sites. Pure ZrO_2 contains only surface acidic sites and the redox sites present on ZrO_2 are inactive under the present ammoxidation reactions conditions (400 °C). Thus, for supported molybdena catalysts, the active surface sites are essentially redox sites as well as the acidic site.

4. Conclusions

Molybdenum oxide catalysts supported on zirconia are found to be highly active in ammoxidation of toluene to benzonitrile. MoO_3/ZrO_2 catalysts were found to exhibit higher activity compared to MoO_3/Nb_2O_5 and MoO_3/TiO_2 catalysts in the ammoxidation of toluene. The activity of the catalysts was found to increase with loading up to 6.6 wt% and the reducibility of the catalysts also increased up to this loading and decreased with a further increase in loading. The best activity and selectivity in the ammoxidation are achieved in the catalyst when the MoO_3 loading is 6.6 wt% and this loading corresponds to monolayer loading. XRD results suggest that below monolayer level MoO_3 exists in a highly dispersed amorphous state and above this loading crystalline MoO_3 can be seen. The acidity of the catalysts also increased up to 6.6 wt% and remained constant at higher loadings. XPS results suggested that only Mo^{6+} and Zr^{4+} are present in the catalysts and did not show any reducible species in the catalysts. It is clear from the XPS results that the dispersion of MoO_3 is high at lower MoO_3 loadings and was found to be low at higher loadings. Laser Raman spectroscopy results suggested that the tetrahedral molybdenum-oxo species is present at lower loadings and the octahedral and crystalline MoO_3 particles are present at higher MoO_3 loading in accordance with XRD data.

Acknowledgments

K.V.R.C. thanks the Royal Society of Chemistry (RSC), UK, for the award of RSC journals grant for international authors. K.R.R. thanks CSIR, New Delhi, for the award of a Senior Research Fellowship. The authors are also grateful to MEL Chemicals, for providing ZrO_2 samples.

References

[1] T. Yamaguchi, Catal. Today 20 (1994) 199.
[2] P.D.L. Mercera, PhD thesis, Twente Institute of Technology, 1991.
[3] H. Miyata, S. Tokuda, T. Ono, T. Ohno, F. Hatayama, J. Chem. Soc., Faraday Trans. 86 (1990) 2291.
[4] K.V.R. Chary, K. Ramesh, G. Vidya sagar, V. Venkat Rao, J. Mol. Catal. 198 (2003) 195.
[5] M. Vrinat, D. Hamon, M. Breysse, B. Durand, T. des Courieres, Catal. Today 20 (1994) 273.
[6] J.G. van Ommen, P.J. Ceilings, J.R.H. Ross, in: D.M. Bibby, C.D. Chang, R.F. Howe, S. Yurchak (Eds.), Methane Conversion, Elsevier, Amsterdam, 1988, p. 213.
[7] Y. Amenomiya, Appl. Catal. 30 (1987) 57.
[8] T. Iizuka, M. Kojima, K. Tanabe, J. Chem. Soc., Chem. Commun. (1983) 638.
[9] H. Miyata, S. Tokuda, T. Ono, T. Ohno, F. Hatayama, J. Chem. Soc., Faraday Trans. 86 (1990) 3659.
[10] K.C. Pratt, J.V. Sanders, V. Christov, J. Catal. 124 (1990) 416.
[11] D. Hamon, M. Vrinat, M. Breysse, B. Durand, M. Jebrouni, M. Roubin, P. Magnoux, T. Des Courieres, Catal. Today 10 (1991) 613.
[12] J.C. Duchet, M. Tillette, D. Cornet, L. Vivier, G. Perot, I. Bekakra, C. Moreau, G. Szabo, Catal. Today 10 (1991) 579.

[13] J.I. Portefaix, M. Cattenot, J.A. Dalmon, C. Mauchausse, in: M.I. Occelli, R.G. Anthony (Eds.), Advances in Hydrotreating Catalysis, Elsevier, Amsterdam, 1989, p. 243.
[14] P. Afanasiev, C. Geanter, M. Breysse, J. Catal. 153 (1995) 17.
[15] E. Iglesia, D.G. Barton, S.L. Soled, S. Miseo, J.E. Baumgartner, W.E. Gates, G.A. Fuentes, G.D. Meitzner, Stud. Surf. Sci. Catal. 101 (1996) 533.
[16] (a) A. Khodakov, J. Yang, S. Su, E. Iglesia, A.T. Bell, J. Catal. 177 (1998) 343;
(b) A. Khodakov, B. Olthof, A.T. Bell, E. Iglesia, J. Catal. 181 (1999) 205;
(c) K. Chen, A. Khodakov, J. Yang, A.T. Bell, E. Iglesia, J. Catal. 186 (1999) 325.
[17] (a) D.S. Kim, K. Segawa, T. Soeya, I.E. Wachs, J. Catal. 136 (1992) 539;
(b) D.S. Kim, I.E. Wachs, K. Segawa, J. Catal. 149 (1994) 268;
(c) K. Segawa, D.S. Kim, Y. Kurusu, I.E. Wachs, in: Proceedings of 9th International Congress on Catalysis, Calgary, Canada, 1960, 1988.
[18] K.V.R. Chary, T. Bhaskar, G. Kishan, V. Vijay Kumar, J. Phys. Chem. 102 (2001) 3936.
[19] K.V.R. Chary, V.V. Kumar, P. Kanta Rao, Langmuir 6 (1990) 1549.
[20] J.A.R. van Veen, P.A.J.M. Hendricks, E.J.G.M. Romers, R.R. Andrea, J. Phys. Chem. 94 (1990) 5275.
[21] (a) J.C. Edwards, P.D. Ellis, Langmuir 7 (1991) 2117;
(b) J.C. Edwards, R.D. Adams, P.D. Ellis, J. Am. Chem. Soc. 112 (1990) 8349.
[22] D.S. Kim, Y. Kurusu, I.E. Wachs, F.D. Hardcastle, K. Segawa, J. Catal. 120 (1989) 325.
[23] K.Y.S. Ng, E. Gulari, J. Catal. 95 (1985) 33.
[24] G. Deo, I.E. Wachs, J. Phys. Chem. 95 (1991) 5889.
[25] F.D. Hardcastle, I.E. Wachs, J. Raman Spectrosc. 21 (1990) 683.
[26] T. Machej, J. Haber, A.M. Turek, I.E. Wachs, Appl. Catal. 70 (1991) 115.
[27] J.M. Stencel, L.E. Makovsky, T.A. Sarkus, J. de Vries, R. Thomas, J.A. Moulijn, J. Catal. 90 (1984) 314.
[28] Y.L. Leung, B.J. Flinn, P.C. Wong, K.A.R. Mitchell, K.J. Smith, Appl. Surf. Sci. 125 (1998) 293.
[29] Y.V. Plyuto, I.V. Babich, I.V. Plyuto, A.D. Van Langeveld, J.A. Moulijn, Appl. Surf. Sci. 119 (1997) 11.
[30] J.G. Choi, L.T. Thompson, Appl. Surf. Sci. 93 (1996) 143.
[31] PJ. Stobbelaar, PhD thesis, University of Eindhoven, 2000.
[32] J. Haber, W. Wojchechowska, J. Catal. 110 (1988) 23.
[33] N.K. Nag, T. Fransen, P. Mars, J. Catal. 68 (1981) 77.
[34] A. Calafat, L. Avilan, J. Aldana, Appl. Catal. 20 (2000) 215.
[35] B. Zhao, X. Xu, H. Ma, D. Sun, J. Gao, Catal. Lett. 45 (1997) 237.
[36] R. Gopalan, C.H. Chang, Y.C. Lin, J. Mater. Sci. 30 (1995) 3075.
[37] P.D.L. Mercera, J.G. van Ommen, E.B.M. Doesburg, A.J. Burgraaff, J.R.H. Ross, Appl. Catal. 78 (1991) 79.
[38] K. Chen, S. Xie, E. Iglesia, A.T. Bell, J. Catal. 189 (2000) 421.
[39] H.Th. Rijnten, PhD thesis, Delft Technical University, 1971.
[40] P. Afanasiev, F. Geantet, M. Breysse, J. Catal. 153 (1995) 17.
[41] S.K. Maity, M.S. Rana, B.N. Srinivas, S.K. Bej, G. Murali Dhar, T.S.R. Prasada Rao, J. Mol. Catal. A: Chem. 153 (2000) 121.
[42] S.C. Su, A.T. Bell, J. Phys. Chem. 102 (1998) 7000.
[43] A.J. van Hengstum, J.G. Van Ommen, H. Bosch, P.J. Ceilings, Appl. Catal. 5 (1983) 207.
[44] R. Thomas, PhD thesis, University of Amsterdam, 1981.
[45] P. Arnoldy, J.C.M. de Jonge, J.A. Moulijn, J. Phys. Chem. 89 (1985) 4517.
[46] J.F. Moulder, W.F. Stickle, P.E. Sobol, K.D. Bomben, Handbook of XPS, Perkin Elmer Corporation, Eden Prairie, MN, 1992.
[47] Y. Iwasawa, S. Ogasawara, J. Chem. Soc., Faraday Trans. I 75 (1979) 1465.
[48] G. Muralidhar, B.E. Concha, G.L. Bartholomew, C.H. Bartholomew, J. Catal. 84 (1984) 274.
[49] N.K. Nag, J. Phys. Chem. 91 (1987) 2324.
[50] H. Shimada, T. Sato, Y. Yoshimura, J. Hiraishi, A. Nishijima, J. Catal. 110 (1988) 275.
[51] C.V. Caceres, J.L.G. Fierro, J. Lazaro, A. Lopez Agudo, J. Soria, J. Catal. 122 (1990) 113.
[52] J.W. Niemantsverdriet, Spectroscopy in Catalysis, MBH Verlaggesellschaft/VCH, Weinheim, 1993.
[53] H. Hu, I.E. Wachs, S.R. Bare, J. Phys. Chem. 99 (1995) 10897.
[54] G. Mestl, T.K.K. Srinivasan, Catal. Rev.-Sci. Eng. 40 (1998) 451.
[55] T. Ono, H. Miyata, Y. Kubokawa, J. Chem. Soc., Faraday Trans. I 83 (1987) 1761.
[56] L. Wang, W.K. Hall, J. Catal. 83 (1983) 242.
[57] Z. Liu, Y. Chen, J. Catal. 177 (1998) 314.
[58] S.S. Chan, I.E. Wachs, L.L. Murrel, L. Wang, W.K. Hall, J. Phys. Chem. 88 (1984) 5831.
[59] K.V.R. Chary, K. Rajender Reddy, Ch. Praveen Kumar, Catal. Commun. 2 (2001) 277.
[60] K.V.R. Chary, K. Rajender Reddy, T. Bhaskar, G. Vidya Sagar, Green Chem. 4 (2002) 206.